Paper 108

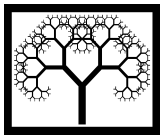

Proceedings of the Eleventh International Conference on Computational Structures Technology,
B.H.V. Topping, (Editor),
Civil-Comp Press, Stirlingshire, Scotland

Vehicle-Bridge Interactive Analyses on the Lagoscuro Viaduct

L. Vincenzi[1], M. Savoia[2] and F. Rossi[3]
[1]DIMEC, University of Modena and Reggio Emilia, Italy
[2]DICAM, Structural Engineering, University of Bologna, Italy
[3]Consorzio Pisa Ricerche, Italy

Abstract

This paper presents the results of dynamic interaction analyses between trains and bridge, with reference to the case-study of the Lagoscuro viaduct. Different vehicle models with varying degrees of sophistication are presented to reproduce more accurately the effects of a train crossing the bridge. The results using the moving loads model and the vehicle-bridge interaction model are compared, and three-dimensional dynamic interaction analyses are performed to study also lateral and torsional vibrations of the Lagoscuro viaduct.

Keywords: vehicle-bridge interaction, dynamic analysis, railway bridge, steel viaduct, contact forces, moving loads.

1 Introduction

The FADLESS research project aims to define innovative technical guidelines for the assessment and control of existing and new bridges with regard to fatigue phenomena induced by vibrations and distortions produced by train passages. The project will employ the most recent experimental and numerical techniques in order to identify the most typical details frequently subjected to high fatigue effects and to draft technical guidelines suitable to control such effects during bridge design or assessment. To identify the most critical details, a fatigue analysis must be performed simulating the vehicle passages and obtain the stress ranges on each element. For this purpose a suitable representation of the vehicle loads is needed.

European guidelines [1] and the actual design codes suggest to represent a vehicle travelling on a bridge by means of a sequence of moving loads. However, with this standard approach, the bridge-vehicle interaction is not taken into account so that some dynamic amplification effects and also movements which generate transverse horizontal forces between the bridge and the wheels of the vehicle are not detected.

The dynamic interaction between a bridge and the moving vehicles represents a special discipline within the structural dynamics field [2]. In order to simulate the train-bridge interactive dynamics many kinds of two-dimensional and three-dimensional models for train carriages have been presented and adopted [3-7], in which the springs and the dashpots are used to describe the interactive effects between wheels and primary suspensions as well as primary and secondary suspensions. The subsystems interact through the contact forces, the forces induced at the contact points between the wheels and the rails surface (of the railway bridge) or the pavement surface (of the highway bridge). Such a problem is nonlinear and time-dependent [8] due to the fact that the contact forces may move from time to time, while their magnitudes do not remain constant, as a result of the relative movement of the two subsystems.

In this paper, vehicle-bridge interaction (VBI) models are reported and results obtained for the Lagoscuro bridge are described. The Lagoscuro viaduct is composed of 2 parallel steel railway viaducts crossing the Po river. The first viaduct was built in 1948 and is composed by 9 single span truss-girder bridges; the upper and the lower chord, diagonals and stunts of the main truss girders are composed of 4 L-shaped steel elements, riveted together by means of plates; stringers and additional elements supporting the railway lines are also riveted. The new Lagoscuro viaduct was recently built in order to potentiate the railway line; the same geometry has been adopted but, differently to the old viaduct, the truss girders are composed by H-shaped elements welded or bolted together in the joints.

In all models, the car bodies, the bogies and the wheels are assumed to be rigid and connected by means of springs and dashpots to represent the two suspensions systems [9-10]. Dynamic analyses will be conducted using a suitable numerical model of the Lagoscuro railway bridge. First, dynamic analyses of the bridge will be performed using the standard procedure given by the Eurocode 1, where the vehicle-bridge interaction is neglected and only a sequence of moving loads is defined, and the results will be compared with those obtained using the 2D VBI model. Then, vehicle-bridge interactive analyses are performed, considering a three dimensional model for cars and bridge. Data regarding the suspensions system of the high-speed train ETR500Y given in [10] will be used.

Figure 1. The Pontelagoscuro viaduct on the Po river.

2 Case study and model setting

The Lagoscuro viaduct consists of 9 steel truss girder bridges with not constant length, crossing the Po river on the Bologna–Venice railway line in the North–East of Italy. Actually the whole structure is formed by 2 railway viaducts running parallel one to each other (Figure 1).

The first viaduct was built in 1948, while the new one has been recently built (2005) in order to potentiate the railway line. The train bridge dynamic interazction is studied with reference to one of the two end side truss girder bridges of the older viaduct, which are 59.4 meters long and 9.60 meters high. Two main truss girders support the vertical load, while X-shaped upper and lower lateral bracing systems assure the transverse stability. The upper and the lower chords, diagonals and stunts consist of 4 L-shaped steel elements, riveted together by means of plates; stiffening plates are also designed to improve the transverse stiffness of the cross-section. Stringers and additional elements supporting the railway lines are also composed of riveted steel elements. End supports are constituted by steel bearings directly in contact with lower main strings, so that a simply supported scheme is realized.

Experimental dynamic tests have been performed in order to identify the modal properties of the bridge in terms of frequencies and mode shapes. The bridge is characterized by a high stiffness in the vertical plane due to the presence of the main truss girders, but it is more deformable in the transverse direction. Therefore, the first mode shape at 2.143 Hz is characterized by horizontal deformation, involving mainly the cross-sections. The second mode shape is a vertical bending mode at 3.857 Hz. The third mode shape (4.307 Hz) is a torsional mode and, finally, the fourth is the second horizontal mode at 4.700 Hz.

A finite elements model of the bridge has been created using four node shell elements (Figure 2). An optimization process is used in order to adjust the modal properties of the FE model and to obtain the numerical predictions as close as possible to the measured data. The identification parameters were the equivalent densities of the lower and upper steel members, in order to take into account all the non–structural masses mainly located at the bottom part of the bridge.

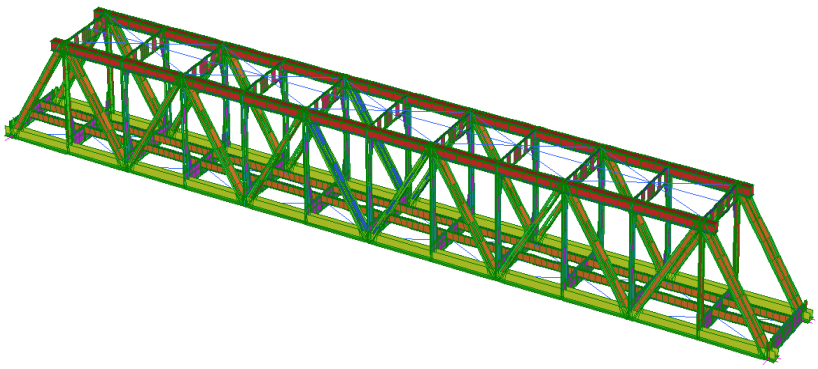

Figure 2. FE model of the bridge

To obtain the unknown parameters, a modified genetic algorithm, developed in [11-12], has been used. In the updating procedure only the first four frequencies and modes shapes have been optimized, obtaining numerical frequencies very close to the experimental values, with errors never greater than 6%, and also a very good mode shapes correlation.

3 Train-bridge dynamic interaction

The most used and widespread method to represent the effects of a vehicle travelling on a bridge is the one obtained by means of a sequence of moving loads. Moreover this method does not take into account the interaction between vehicle and bridge. Vehicle models with a varying degree of sophistication can be found in literature (see for instance [4,5,8]) to account for the dynamic effect between train and bridge. Possible planar models consisting of masses supported by springs and dashpots that could be used in the two-dimensional analyses are those given in reference [9]. For this kind of vehicle models, a set of ordinary differential equations of motion can be written as:

$$\mathbf{M}_v \ddot{\mathbf{v}}_v + \mathbf{C}_v \dot{\mathbf{v}}_v + \mathbf{K}_v \mathbf{v}_v = \mathbf{P}_v \tag{1}$$

where $\mathbf{M}_v$, $\mathbf{C}_v$ and $\mathbf{K}_v$ are the mass, damping and stiffness matrices; $\mathbf{v}_v$, $\dot{\mathbf{v}}_v$ and $\ddot{\mathbf{v}}_v$ are the displacement, velocity and acceleration vectors of the vehicle system; and $\mathbf{P}_v$ is the vector that collects the dynamic force on the vehicle. Without loss of generality, the terms in Equation (1) can be specialized for a 3–DOFs vehicle model of Figure 3. The mass matrix of the vehicle can be written as:

$$\mathbf{M}_v = diag\left[M_1, M_2, M_1\right] \tag{2}$$

where M_1 and M_2 are the masses of the bogies and of the car body respectively. The stiffness matrix can be written as:

$$\mathbf{K}_v = \begin{bmatrix} 2K_V + K_{VV} & -K_{VV} & 0 \\ -K_{VV} & 2K_{VV} & -K_{VV} \\ 0 & -K_{VV} & 2K_V + K_{VV} \end{bmatrix} \tag{3}$$

with the meaning of the terms specified in Figure 3. The damping matrix can be obtained just replacing the stiffness terms K_V, K_{VV} with the damping terms C_V and C_{VV} of the primary and secondary suspension system. $\mathbf{P}_v$ is function of the wheels displacements and velocities and can be obtained as:

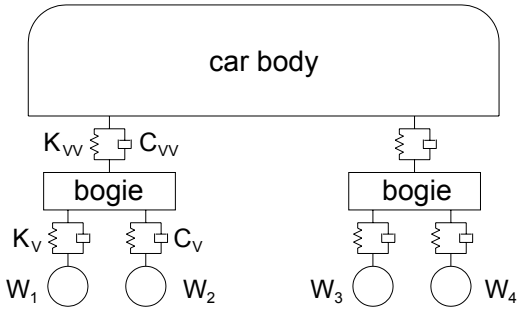

Figure 3. 3–DOFs vehicle model

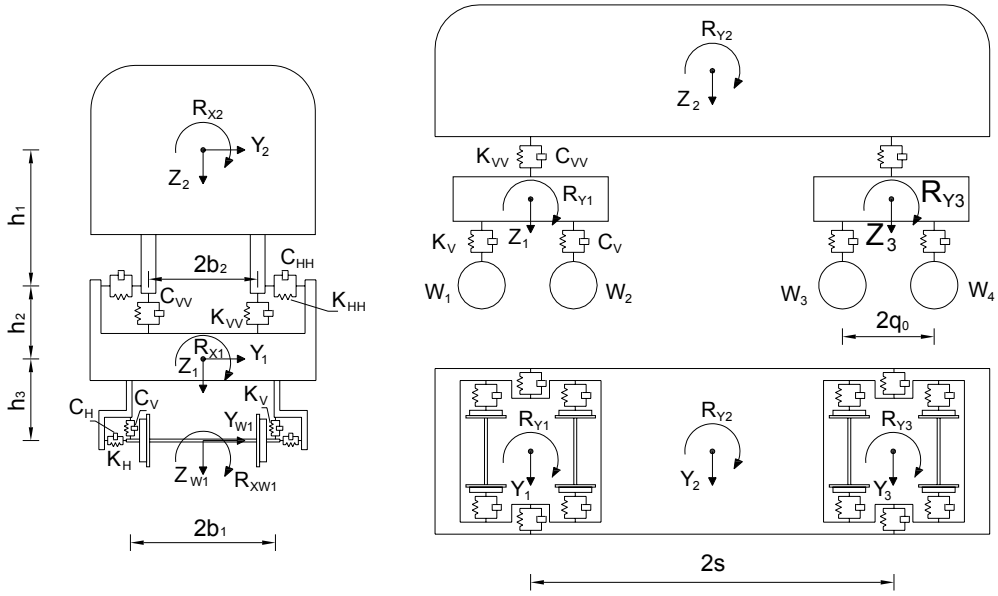

Figure 4. Vehicle models with 15 DOFs [10]

$$\mathbf{P}_v = \begin{bmatrix} K_V\left(V_{W1}+V_{W2}\right)+C_V\left(\dot{V}_{W1}+\dot{V}_{W2}\right) \\ 0 \\ K_V\left(V_{W3}+V_{W4}\right)+C_V\left(\dot{V}_{W3}+\dot{V}_{W4}\right) \end{bmatrix} \tag{4}$$

since first and second axles (subscript 1 and 2) are connected to the front bogie and the third and fourth axles (subscript 3 and 4) to the rear bogie.

A more sophisticated vehicle model represented in Figure 4, proposed in [10], can be used to perform three–dimensional analyses. Using this model also horizontal and torsional modes can be involved and studied. The equation of motion can still be represented by the Equation (1); more details are given in [10,13]. A set of ordinary differential equations of motion can be written to represent the dynamic behaviour of the bridge as:

$$\mathbf{M}_b \ddot{\mathbf{v}}_b + \mathbf{C}_b \dot{\mathbf{v}}_b + \mathbf{K}_b \mathbf{v}_b = \mathbf{P}_b \tag{5}$$

where $\mathbf{M}_b$, $\mathbf{C}_b$ and $\mathbf{K}_b$ are the mass matrix, damping matrix and stiffness matrix, respectively; $\mathbf{v}_b$, $\dot{\mathbf{v}}_b$ and $\ddot{\mathbf{v}}_b$ represent the displacement, velocity and acceleration vectors of the bridge DOFs, and $\mathbf{P}_b$ is the force vector transferred to the bridge.

In some finite elements models, thousands of nodes and elements are used, therefore the Equation (5) could be a system of thousands equations. Due to the fact that it is often possible to describe an approximate dynamic response with just a few modes, the system of equations can be substantially reduced. In fact, rewriting the equations of motion in modal coordinates and normalizing the mode shapes in respect to the mass matrix, the set of equations assume the following form:

$$\ddot{\mathbf{q}}_b + \mathbf{C}_b^* \dot{\mathbf{q}}_b + \mathbf{K}_b^* \mathbf{q}_b = \mathbf{P}_b^* \tag{6}$$

where the matrices $\mathbf{C}_b^*$, $\mathbf{K}_b^*$ and the vector $\mathbf{P}_b^*$ are defined as follows:

$$\mathbf{C}_b^* = 2\xi\boldsymbol{\Omega}; \quad \mathbf{K}_b^* = \boldsymbol{\Omega}^{2;} \quad \mathbf{P}_b^* = \Phi^T \mathbf{P}_b \tag{7}$$

and Φ is the $N_{DOF} \times N_0$ mode shapes matrix and $\boldsymbol{\Omega}$ is the $N_0 \times N_0$ diagonal matrix that collects the frequencies of the considered modes. $\mathbf{P}_b$ is determined knowing the position along the bridge of the wheel axles at each time step. In this case the first four optimized modes are considered to describe the motion of the bridge, so that Equation (6) results in a set of four uncoupled equations.

When considering a 3–DOF vehicle model (Figure 3), the equivalent nodal force vector $\mathbf{P}_b$ transferred to the bridge can be computed as:

$$\mathbf{P}_b(t) = \sum_{i=1}^{4} \mathbf{y}_i(t) F_{Gi} + \sum_{i=1}^{4} \mathbf{y}_i(t) \left[-M_{Wi} \ddot{\mathrm{v}}_{Wi} + K_V \left(\mathrm{v}_j - \mathrm{v}_{Wi} \right) + C_V \left(\dot{\mathrm{v}}_j - \dot{\mathrm{v}}_{Wi} \right) \right] \tag{8}$$

where $\ddot{\mathrm{v}}_{wi}$ represents the acceleration of the i^{th} wheel set; v_j represents the displacement of the bogie and M_{Wi} and F_{Gi} represent the mass and the quasi–static part of the load of the i^{th} wheel set, respectively. The vector $\mathbf{y}(t)$ is the $N_{DOF} \times 1$ vector that transfers a moving unit load to equivalent nodal forces according to the position of the i^{th} axle.

The vehicle–bridge dynamic interaction problem can be solved with an iterative procedure within each time step coupling the two sets of equations enforcing compatibility conditions in terms of displacements at the contact points.

$$\begin{cases} \ddot{\mathbf{q}}_b + \mathbf{C}_b^* \dot{\mathbf{q}}_b + \mathbf{K}_b^* \mathbf{q}_b = \mathbf{P}_b^* \\ \mathbf{M}_v \ddot{\mathbf{v}}_v + \mathbf{C}_v \dot{\mathbf{v}}_v + \mathbf{K}_v \mathbf{v}_v = \mathbf{P}_v \end{cases} \tag{9}$$

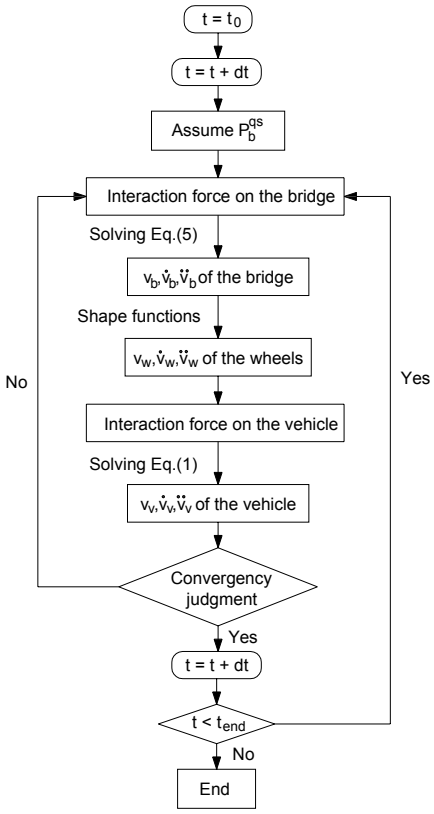

Figure 5. Flowchart of the solving procedure

The equations of motions are solved using Newmark's method. The iterative procedure is shown in details in Figure (5). Therefore, assigning a time step Δt and knowing the velocity v, the weight W and the relative distances of all the axles of each train, Equation (9) can be solved. Then the interaction forces on the bridge and on the vehicle can be computed for each time step, and so nodal loads time history can be obtained. Furthermore, accelerations, velocities and displacements time history for each degree of freedom both for bridge and vehicle can be calculated for the given crossing train.

4 Results

In this section the dynamic analyses of the bridge will be shown using three different representations of the crossing trains. The first train model is defined as a loads sequence (*moving loads model*), according to Eurocode 1; the second one is a sequence of 3–DOFs cars (Figure 3) with the same weight of standard trains defined in Eurocode. Due to the symmetric load condition, 2D VBI model and moving loads model are unable to excite members as lower bracing. The 3D VBI model is then introduced to obtain also interaction in the transverse direction. In order to perform

the 3D VBI analysis, values of the vertical stiffness and vertical damping of the primary and secondary suspension systems are needed. In literature there are very scarce data about the values of these devices. Therefore the data about the Italian ETR500Y high–speed train given in [10] will be used for each type of train.

Figures 6 and 7 compare the displacements time history at mid span node obtained using the moving load model and the 2D VBI model for Train type 1 and 2 and Train type 3 and 9, respectively. Small differences between the two train models are obtained during the train passage and in the free vibrations after the train has left the bridge. The maximum displacement of the bridge is about 25 mm for the moving loads model and 27 mm for the VBI model when the train type 1 crosses the bridge. Similar results can be obtained for all passengers trains (see for instance train type 2 – Figure 6*b*).

Some representative results obtained with the 3D VBI model are shown in Figure 8 for equivalent train Type 5 and 7. As shown, the 3D VBI model is able to obtain also a dynamic interaction between the cars and the bridge in the horizontal direction.

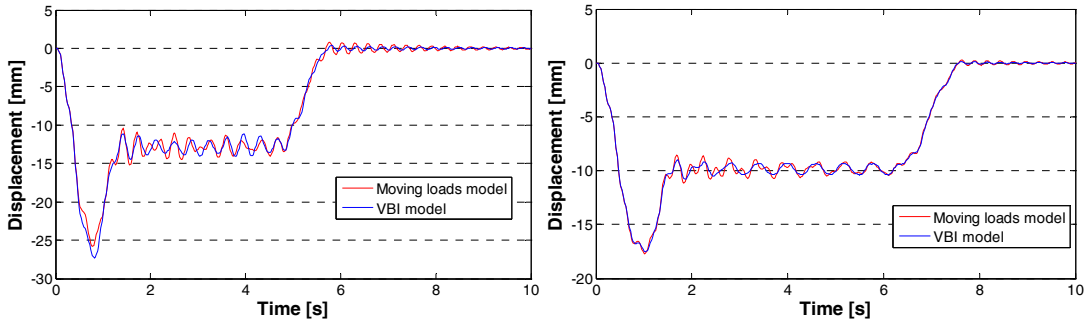

Figure 6. Comparison between moving loads and 2D VBI models for (*a*) train type 1 and (*b*) train type 2

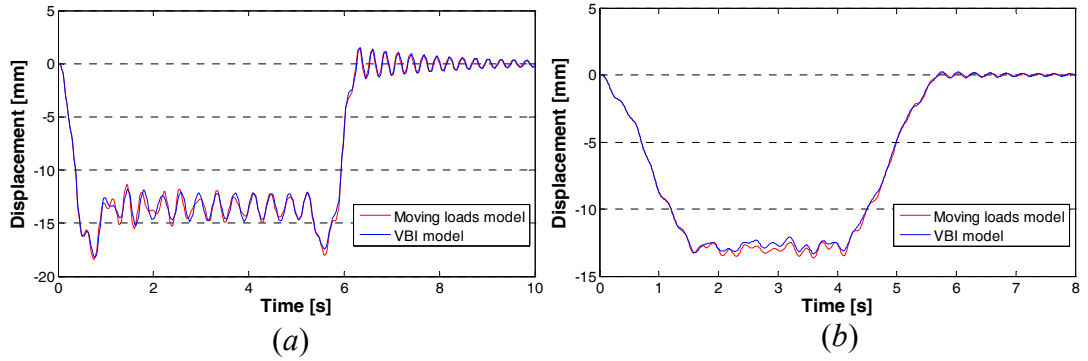

Figure 7. Comparison between moving loads and 2D VBI models for (*a*) train type 3 and (*b*) train type 9

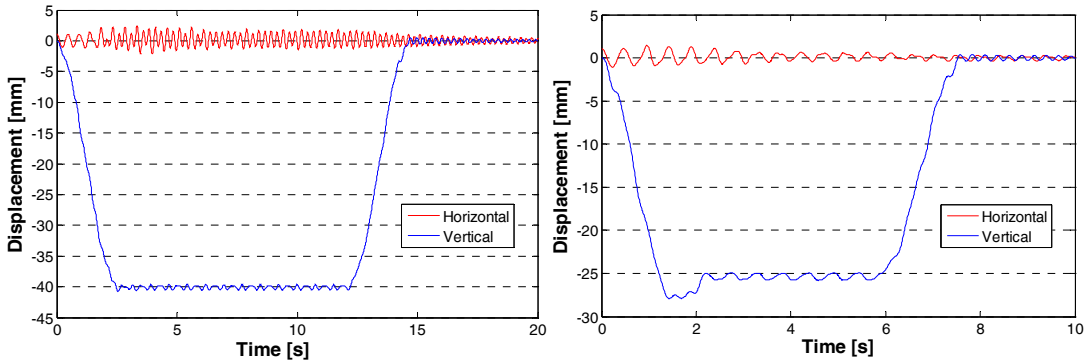

Figure 8. 3D VBI analyses: horizontal and vertical displacement for (*a*) train type 5 and (*b*) train type 7

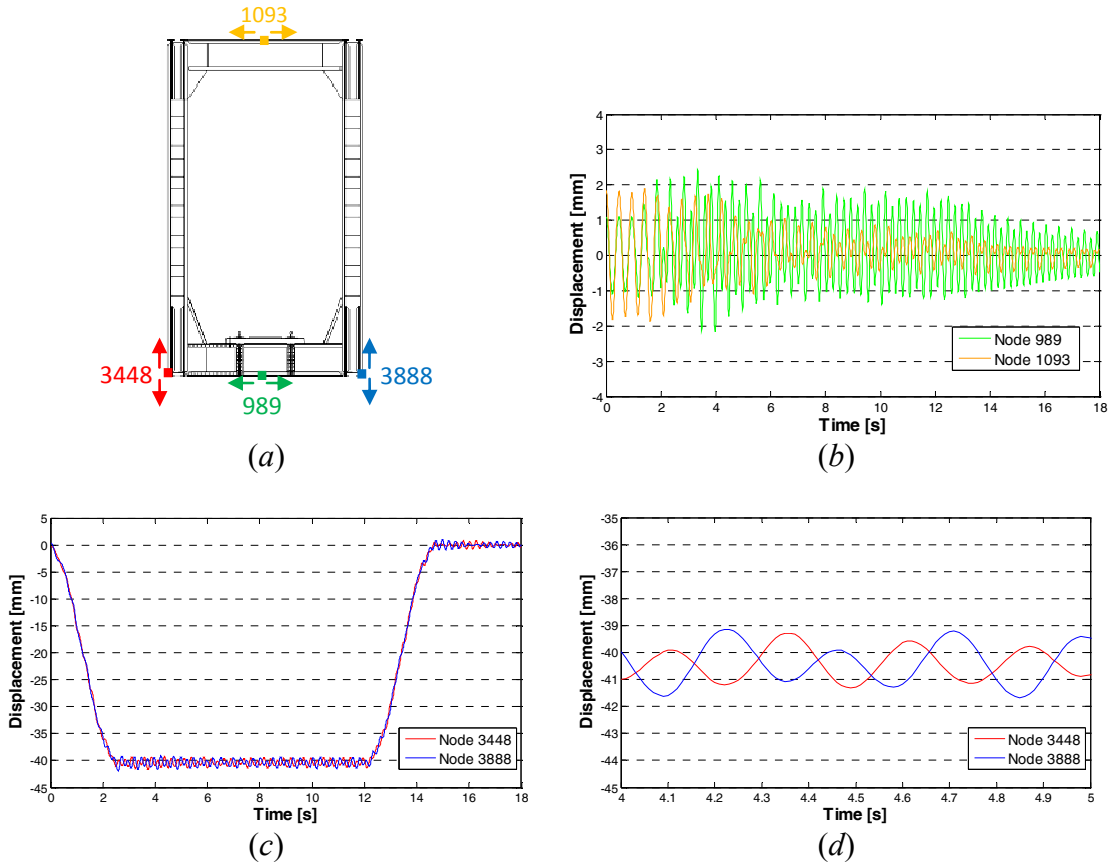

Figure 9. (*a*) Bridge transversal cross–section; (*b*) horizontal displacement time history of the nodes 989 and 1093; (*c*) vertical displacement time history of the nodes 3448 and 3888; (*d*) lower scale view of (*c*)

To excite horizontal and torsional modes, dynamic analyses are carried out imposing a initial condition (displacement) to the bridge. As expected, very small oscillations amplitude is obtained in the horizontal direction, being the railway track centred in

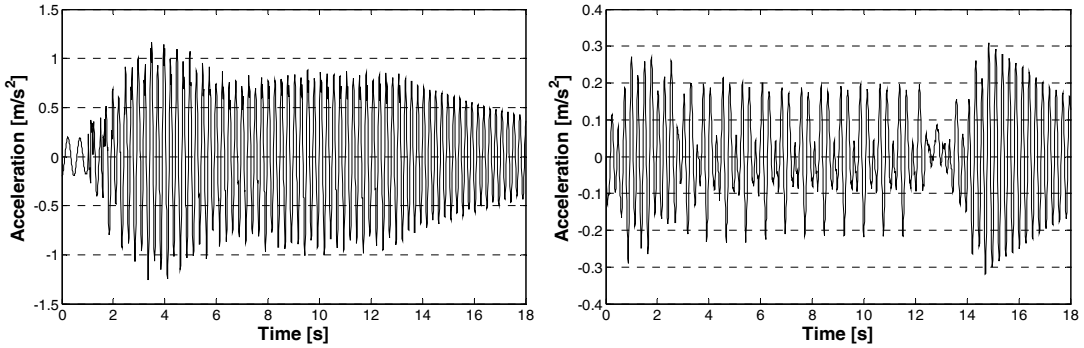

Figure 10. (*a*) horizontal acceleration time history and (*b*) vertical acceleration time history of the mid span node of the bridge

respect to the axis of the bridge, but sufficient to load the X bracings and to excite the torsional mode shape. In order to better understand the dynamic behaviour of the mid span transversal cross-section of Figure 9*a*, the horizontal time history displacement of the nodes 989 and 1093 and the vertical time history displacement of the nodes 3448 and 3888 regarding the train type 5 are plotted in Figure 9*b* and 9*c*, respectively. Figure 9*d*, where a lower scale view of Figure 9*c* is presented, shows the counter phase motion of the nodes 3448 and 3888 suggesting that torsional vibration is involved. In Figure 10 the horizontal and vertical acceleration time histories of the lower mid span node 989 of the bridge (see Figure 9*a*) due to the passage of the freight train type 5 are shown. Higher values of the accelerations are predicted in the horizontal direction with values bounded between 1.2 and -1.2 m/s^2, in comparison to the accelerations in the vertical direction which are included within 0.3 and -0.3 m/s^2. In further works, the obtained results will be compared with the experimental acceleration time histories acquired during the transit of a similar train.

Also the dynamic response of the vehicle can be obtained and studied performing vehicle-bridge dynamic interaction analyses. Figures 11*a* and 11*b* show respectively the computed vertical displacement and acceleration time histories of the car body of the ETR500Y Italian high speed train when it crosses the bridge. Masses and suspensions characteristics given in [10] and reported in Appendix A are used. Therefore with this method even the passengers travelling comfort could be studied, especially in the design phases of a new bridge construction.

As regards the train-bridge dynamic interaction problem, many parameters influence the dynamic behavior of the bridge. For this reason in Figure 12 the influence of the train velocity on the bridge response is investigated. Dynamic analyses are carried out for velocities in the range of 10–400 km/h with a step of 5 km/h. According to [10], the critical speed at which dynamic amplification arise can be computed as:

$$V_{cri} = \frac{l_0}{i} \cdot f_n \tag{10}$$

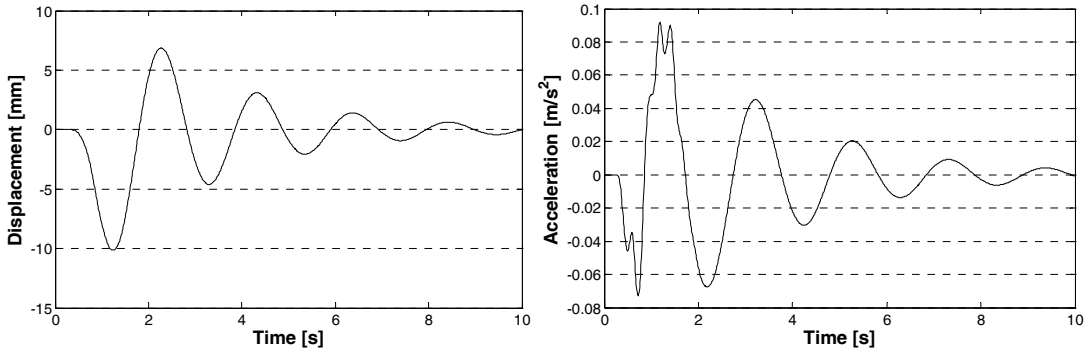

(a) (b)

Figure 11. (a) vertical displacement time history and (b) vertical acceleration time of the car body of the ETR 500Y high speed train

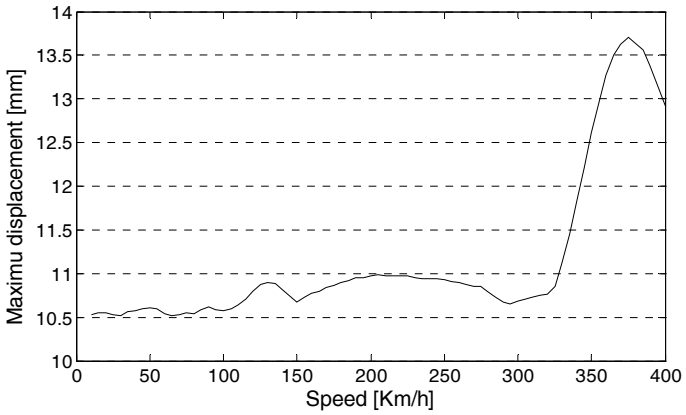

Figure 12. Maximum displacement of the mid span node 989 for different train speeds

with $i = 1,2,3,...,n$.

For the high–speed train ETR500Y, $l_0 = 26.1$ m, $i = 1$ and the first bending frequency of the bridge is $f = 3.857$ Hz. The critical speed is 362 Km/h that is in agreement with the analysis.

A parametric investigation has been conducted changing the weight of the ETR500Y train, and so varying the mass properties of the cars. Performing dynamic analyses going from halved value to double value of the mass, not significant results have been obtained, and the bridge response is essentially linear with the weight increasing, so confirming that the interaction between bridge and vehicle is negligible.

5 Conclusion

In this paper an advanced method aimed at performing dynamic analyses of bridges has been used to describe the effects of the dynamic interaction between vehicle and bridge. Dynamic analyses have been conducted on the Lagoscuro viaduct. First of all two approaches are used and compared to represent the effects of a train crossing on the bridge response, by means of a sequence of moving loads and by means of a series of 2D VBI cars model, for some trains given by the Eurocode 1 for fatigue analysis. From these analyses only very small differences are detected in the values of the peaks of the displacement time history.

Performing 3D VBI analyses also lateral and torsional effects have been obtained and studied. Then parametric investigations have been conducted as regard the travelling speed and the weight of the train.

Afterwards, the obtained results will be validated and compared with the experimental records that will be acquired through in situ measurements for similar train types.

Acknowledgements

The research was developed in the framework of the FADLESS research project (Fatigue Damage Control and Assessment for Railway Bridges). Financial supports of European Commission - RFCS (Research Fund for Coal and Steel) is gratefully acknowledged.

The second author is presently a fellow of the Italian Academy of the Columbia University in New York: the support of the Italian Academy if gratefully acknowledged.

References

[1] Eurocode 1, “Actions on structures – Part 2: Traffic loads on bridges”, European committee for standardization, EN 1991-2, 2003.

[2] L. Fryba. “Dynamics of railway bridges”. London: Thomas Telford; 1996.

[3] F. Yang, G.A. Fonder. “An iterative solution method for dynamic response of bridge-vehicles systems”. Earthquake Eng Struct Dynam 25, 195–215, 1996.

[4] Y.B. Yang, B.H. Lin. “Vehicle-bridge interaction analysis by dynamic condensation method”. J Struct Eng, 121(11), 1636–43, 1995.

[5] Y.S. Cheng, F.T.K. Au, Y.K. Cheung. “Vibration of railway bridges under a moving train by using bridge–track–vehicle element”. Eng Struct 23, 1597–606, 2001.

[6] Q. Zhang, A. Vrouwenvelder, J. Wardenier. “Numerical simulation of train-bridge interactive dynamic”, Computer and Structure 79: 1059-1075, 2001.

[7] Y.S. Wu, Y.B. Yang. “Steady-state response and riding comfort of trains moving over a series of simply supported bridges”. Eng Struct 25, 251–65, 2003.

[8] B. Biondi, G. Muscolino, A. Sofi. “A substructure approach for the dynamic analysis of train-track-bridge system”, Computer and Structure 83: 2271-2281, 2005.
[9] K. Liu, G. De Roeck, G. Lombaert, “The effect of dynamic train-bridge interaction on the bridge response during a train passage”, Journal of Sound and Vibration 325, Elsevier, 2009.
[10] K. Liu, E. Reynders, G. De Roeck, G. Lombaert, “Experimental and numerical analysis of a composite bridge for high-speed trains”, Journal of Sound and Vibration 320, Elsevier, 2008.
[11] M. Savoia, L. Vincenzi, “Differential evolution algorithm for dynamic structural identification”, Journal of Earthquake Engineering,12:800-821, 2008.
[12] L. Vincenzi, M. Savoia, “Improving the speed performance of an evolutionary algorithm by second-order cost function approximation”, 2nd International Conference on Engineering Optimization, September 6-9, 2010, Lisbon, Portugal.
[13] K. Liu, E. Reynders, G. De Roeck,”Experimental validation of the dynamic interaction analysis between high-speed trains and the Sesia viaduct”, Leuven University, Belgium.

Appendix A

Characteristics of EYR500Y high-speed train [3].

Item	Unit	Locomotive	Passenger car
Mass of car body (M_2)	Kg	55976	34231
Mass moment of inertia of car body around x-axis (I_{x2})	Kg·m^2	53366	54642
Mass moment of inertia of car body around y-axis (I_{y2})	Kg·m^2	1643086	1821521
Mass moment of inertia of car body around z-axis (I_{z2})	Kg·m^2	1630520	1760619
Mass of bogie (M_1)	Kg	3896	2760
Mass moment of inertia of bogie around x-axis (I_{x1})	Kg·m^2	3115	2304
Mass moment of inertia of bogie around y-axis (I_{y1})	Kg·m^2	2059	2504
Mass moment of inertia of bogie around z-axis (I_{z1})	Kg·m^2	8107	4071
Mass of wheel set (M_w)	Kg	2059	1583
Mass moment of wheel set (I_w)	Kg·m^2	1164	753
Lateral stiffness of the primary suspension system (K_H)	N/m	82821	3750
Vertical stiffness of the primary suspension system (H_V)	N/m	896100	404370
Lateral damping of the primary suspension system (C_H)	N·s/m	0	0
Vertical damping of the primary suspension system (C_V)	N·s/m	7625	3750
Vertical stiffness of the secondary suspension system (K_{HH})	N/m	73035	32054
Vertical stiffness of the secondary suspension system (K_{VV})	N/m	236030	90277
Lateral damping of the secondary suspension system (C_{HH})	N·s/m	4625	5000
Vertical damping of the secondary suspension system (C_{VV})	N·s/m	18125	8125
Half distance between two wheel-sets (q_0)	m	1.5	1.5
Half span of the primary suspension system (b_1)	m	1.115	0.965
Half span of the secondary suspension system (b_2)	m	1.0425	1.0825
Car body and the secondary suspension system distance (h_1)	m	0.915	0.7
Secondary suspension system and bogie distance (h_2)	m	0.098	0.12
Bogie and wheel sets distance (h_3)	m	0.087	0.13